Brain Stimulation 18 (2025) 770–779

Contents lists available at ScienceDirect

Brain Stimulation

journal homepage: www.journals.elsevier.com/brain-stimulation

Subjective patient rating as a novel feedback signal for DBS programming in Parkinson's disease

Jing Dong [a], Sophia Peschke [a], Angelina Kirschner [a], Carla Palleis [a,b], Jan Hinnerk Mehrkens [c], Maximilian Scherer [a], Elisabeth Kaufmann [a], Thomas Koeglsperger [a,b,*]

[a] Department of Neurology, LMU University Hospital, LMU Munich, Munich, Germany
[b] Department of Translational Brain Research, German Center for Neurodegenerative Diseases (DZNE), Munich, Germany
[c] Department of Neurosurgery, LMU University Hospital, LMU Munich, Munich, Germany

ARTICLE INFO

Keywords:
Visual analogue scale (VAS)
Parkinson's disease (PD)
Deep brain stimulation (DBS)
Connectomics

ABSTRACT

Background: Deep brain stimulation of the subthalamic nucleus (STN-DBS) effectively alleviates motor fluctuations in Parkinson's disease (PD). Optimal electrode placement and effective programming significantly influence outcomes. From a patient's perspective, DBS should relieve motor symptoms while avoiding side effects. However, there is a lack of programming routines that consider patients' subjective feedback for parameter adjustment.

Objective: This study assessed the usefulness of patients' subjective ratings as feedback for DBS programming.

Methods: We analyzed 260 DBS settings from 11 STN-DBS patients, pairing each volume of tissue activated (VTA) with a subjective rating measured by a visual analogue scale (VAS). We performed sweet spot mapping and connectivity analyses, utilizing voxel-wise and nonparametric permutation statistics to identify neuroanatomical regions and connectivity profiles associated with the highest VAS ratings. To validate our findings, we cross-validated the results in an independent test dataset of 6 patients (189 settings) to determine if the sweet spot and connectivity profile could predict the subjective patient perception.

Results: VTAs with the highest VAS scores were localized to the dorsolateral STN, consistent with published sweet spots derived from clinical data. Connectivity with the supplementary motor area (SMA) and primary motor cortex (M1) was associated with a more positive subjective perception. Connectivity profiles derived from one dataset successfully predicted outcomes in an independent dataset, as validated through leave-one-cohort-out cross-validation.

Conclusions: Mapping patients' subjective perceptions using VAS yields conclusive anatomical results that align with objective clinical and imaging measures. VAS-guided programming could provide an additional feedback mechanism for both acute and chronic DBS parameter adjustments.

1. Introduction

Deep brain stimulation (DBS) is the preferred treatment for advanced Parkinson's disease (PD), essential tremor (ET), and complex segmental and generalized dystonia. Successful treatment outcomes depend on careful patient selection, precise electrode placement, and effective DBS programming [1,2]. Among these, DBS programming is the only factor that can be modified postoperatively, making it especially crucial whenever electrodes are not optimally implanted. Additionally, DBS programming plays a key role in treatment success and patient satisfaction [3,4].

Despite several clinical strategies for adjusting neurostimulation [5], DBS programming remains time- and resource-consuming [6]. Consequently, there is a demand for innovative approaches to adjust stimulation parameters and lead configurations quickly, precisely, and effectively. Disease-specific biomarkers are currently being examined, which can be integrated into adaptive closed-loop stimulation systems (aDBS) that respond to real-time patient needs and obviate the need for manual programming [7]. Besides clinical approaches based on motion sensors [8] and imaging-guided programming methods [9–17],

* Corresponding author. Department of Neurology, LMU University Hospital, LMU Munich, Marchioninistr. 15, 81377, Munich, Germany.
E-mail address: thomas.koeglsperger@med.uni-muenchen.de (T. Koeglsperger).

https://doi.org/10.1016/j.brs.2025.03.008
Received 18 August 2024; Received in revised form 24 February 2025; Accepted 9 March 2025
Available online 11 March 2025

oscillatory activity in the beta frequency band (13–30 Hz) has been suggested as an electrophysiological feedback signal for aDBS [18–25].

Despite recent technological advancements aimed at optimizing motor symptoms, current DBS programming routines [5,7] lack the methodology to capture the patient's subjective perspective on treatment efficacy. From a patient's viewpoint, overall satisfaction with DBS depends not only on the clinical effectiveness in alleviating motor symptoms but also on the avoidance of DBS-associated motor and non-motor side effects. These findings emphasize the need to incorporate additional feedback signals into aDBS protocols to ensure they account for patient perceptions [26–28]. Ideally, such protocols could serve as supplementary approaches for remote programming, when traditional clinical signals are either inapplicable or can only be tested to a limited extent [29].

Previously, we examined the significance of patients' subjective feedback measured by a visual analogue scale (VAS) and found no notable short-term difference between VAS-based and traditional programming approaches in terms of specific contact or amplitude used, nor in relation to clinical disease severity as assessed by the Unified Parkinson's Disease Rating Scale (UPDRS) [30]. This suggests the potential for VAS-based programming strategies as an alternative DBS programming approach. Yet, it remains uncertain whether the stimulation of specific brain regions is linked to a positive or negative subjective perception of DBS efficacy. In this study, we therefore employed MRI-based analytical tools to identify "subjective sweet spots" within the STN target area, guided by patient-reported VAS ratings. To achieve this, we conducted sweet spot mapping and connectivity analyses, using voxel-wise and nonparametric permutation statistics to pinpoint neuroanatomical regions and connectivity patterns associated with the best patient rating.Klicken oder tippen Sie hier, um Text einzugeben.

2. Subjects and methods

Study Participants: Detailed information regarding the study visits and programming procedures were previously published in Ref. [30]. All study-associated procedures have been approved by the local ethics committee at Ludwig Maximilian University of Munich, Germany (#18–809) and written informed consent has been obtained from all study participants. PD patients who underwent DBS of the STN were recruited from routine visits at our movement disorder outpatient clinic. Participants were selected based on their interest in participating and meeting main inclusion criteria, including a PD diagnosis and STN-DBS according to the Movement Disorder Society (MDS) criteria. Additionally, participants had undergone DBS for at least one year and were on a stable DBS program for at least three months prior to this study visit, without severe cognitive impairment or significant neuropsychiatric issues. All patients were examined in a pharmacological MED-ON state, without pausing any medication prior to the study visit.

Study Visit and VAS Rating: We first determined the UPDRS III (UPDRS-Pre) in the MED ON/STIM-ON state at the start of the study visit, chronic stimulation parameters were documented, and the stimulation for the clinically predominant side turned off thereafter. Patients were then asked to rest for 30 min before the UPDRS III in MED-ON/STIM-OFF state was measured again (UPDRS-Off). Afterward, all patients underwent VAS-based reprogramming of their stimulator on the side that had been switched off. VAS sampling was conducted during the MED ON state. DBS was applied iteratively across all DBS contacts/ring levels of the corresponding lead, ranging from 0.5 to 3.5 mA in 0.5 mA increments. The various DBS program settings (contacts and amplitudes) were explored in a randomized manner to prevent habituation. Randomization has been achieved via a computer tool. For each adjustment, the patient had up to 30 s to rate their satisfaction with the current DBS program on a scale from 0 (very bad) to 10 (very good). We instructed all participants to consider not only motor symptoms but also other aspects they could perceive, such as mood, sense of well-being, and the presence or absence of side effects. This approach aimed to encourage an integrated rating that reflects their overall sense of benefit or discomfort from the stimulation settings. The respective VAS rating was documented, and the next adjustment was made manually. The UPDRS III (UPDRS-Post) in "MED ON/STIM-ON" state, under the VAS-derived DBS program, was conducted before switching back to the original settings. Throughout the adjustment process, all patients were blinded to the stimulator settings. A 60-s "washout" period [31] was maintained after each VAS setting before presenting the next one. During clinical testing, VAS ratings from stimulation settings that caused intolerable side effects were excluded. For instance, if strong side effects were produced by a given contact at 2.5 mA, the patient was not queried at 3 mA for the same contact. The overall VAS-based adjustment process took approximately 45 min per patient. The patient's baseline motor symptoms remained consistent throughout the trial (Fig. S1e). Given the subjective nature of these ratings, VAS scores were normalized using z-scores prior to further analysis to ensure consistency and reliability.

Training Dataset (Dataset #1): The initial dataset included 11 PD patients who had undergone bilateral STN-DBS at LMU University Hospital, and their characteristics had been previously published. DBS was administered to these patients using varying amplitudes (ranging from 0.5 to 3.5 mA in 0.5 mA increments) from each ring of the DBS lead. In cases where patients had segmented DBS leads, segments were activated simultaneously to mimic ring activation, resulting in 28 distinct combinations for each patient. After excluding DBS programs that caused significant side effects, the final dataset comprised 260 stimulation settings sampled from 11 patients.

Test Dataset (Dataset #2**):** The second dataset consisted of 6 PD patients who underwent bilateral STN-DBS at LMU University Hospital using similar devices. Data acquisition was mostly equal in this cohort with two exceptions: Each contact was tested separately for patients with segmented electrodes. DBS programs at 3.5 mA were not explored as these induced considerable stimulation related side effects in the training dataset.

Localization of DBS Leads: Preoperative T1-weighted and T2-weighted MRI scans, as well as postoperative CT scans, were used for image processing for each patient. Electrode localization was performed using the Lead-DBS toolbox (lead-dbs.org) [32]. Specifically, preoperative MRI and postoperative CT scans were linearly co-registered using Advanced Normalization Tools (ANTs). The native patient images were then normalized into the Montreal Neurological Institute (MNI) space through a three-step affine normalization process using ANTs, with further refinement of the atlas fit as needed. The brain bias (brain shift) with respect to the skull caused by postoperative pneumocephalus resulting from the surgical procedure was corrected using the brain shift correction setting in Lead-DBS. The registration was manually verified. Electrode trajectories were pre-reconstructed using the PaCER algorithm [33] and manually optimized on a case-to-case basis. For directional leads, rotation was identified using the DiODe algorithm [31]. The DISTAL atlas [34] was used as the basis for defining atlas segmentations in this study.

Volume of Tissue Activated (VTA) Estimation: VTAs were calculated using the Finite Element Method (FEM)-based VTA model implemented in Lead-DBS. Subcortical gray matter nuclei were defined by the DISTAL atlas, with conductivities set at 0.33 S/m for gray matter and 0.14 S/m [35] for white matter. E-fields were calculated using the SimBio/FieldTrip pipeline in Lead-DBS to determine the extent and shape of the VTAs, applying a threshold of $e = 0.2V/mm$, commonly used in similar contexts [36]. A VTA was then created for each setting and paired with a specific VAS rating.

Sweet Spot Analysis: Sweet-spot mapping utilized Sweetspot Explorer from Lead DBS to pinpoint neuroanatomical regions within the STN that corresponded to subjective patient ratings. VTAs (Volume of Tissue Activated) were thresholded with an E-fields magnitude above 0.2V/mm, and voxels covered by at least 20 % of VTAs were included in the analyses [32,36]. Subsequently, VTAs from the left hemisphere were mirrored to the right hemisphere using non-linear transformation. Each

voxel was then paired with the Visual Analog Scale (VAS), and the cumulative contribution of VTAs along with their mean VAS values were computed for each voxel. Mean-effects images were generated post z-score normalization of the data. Voxel-wise parametric permutation statistics were applied, testing against zero to identify statistically significant outcomes. After applying z-score normalization to the data, voxel-wise statistics were performed using a *t*-test, tested against zero to identify voxels significantly higher or lower than zero. The amplitudes were adjusted to mitigate the greater influence of higher amplitudes on stimulation maps, as these affect more voxels. For further analysis, only voxels displaying significant positive or negative results ($p < 0.05$) were considered part of the sweet spot or sour spot [37]. To assess effectiveness and reliability, Lead-DBS' leave-one-patient- and leave-one-cohort-out strategy was employed for cross-validation purposes. In addition, and 5-fold and 10-fold cross-validation was performed as described [38].

Connectivity Estimation: To investigate the connectivity network model associated with VAS, whole-brain structural and functional connectivity seeding from bilateral VTA were calculated using two connectomes. Structural connectome data were derived from diffusion MRI (dMRI) of 85 patients from the Parkinson's Progression Markers Initiative (PPMI) database [39]. The PPMI database includes data from 90 patients (mean age ± SD: 61.38 ± 10.42 years; 31 % female) (www.ppmi-info.org). Our combined dataset consists of patients with a mean age of 63.91 ± 7.62 years and 23.52 % female, closely matching the PPMI cohort in terms of age and sex. Analysis for structural connectivity involved performing whole-brain tractography for each patient, normalizing tracts, and aggregating tracts across patients. Functional connectome data were derived from 74 PPMI PD-patients and 15 controls, with global signal regression and spatial smoothing applied (PPMI connectome). Based on different interactive connectivity models for predicting clinical outcomes, A-maps (weighted average maps), R-maps (correlation maps between VTA connectivity and VAS), and C-maps (combined maps) were created [40]. These connectivity maps were then analyzed using Spearman rank correlation with VAS values in a voxel-wise manner, resulting in maps that indicated positive or negative correlations with subjective patient ratings. The Human Connectome Project (HCP) connectome [41] or PPMI-75 connectome [42] were used as templates for validation purposes.

3. Results

3.1. Patients and clinical outcomes

Our study included a total of 17 patients who underwent STN-DBS treatment, divided into two separate datasets (Table 1). Among them, four were female, with a mean age of 63.91 ± 7.62 years. The average disease duration for the entire group was 14.65 ± 3.57 years, and the average duration of DBS treatment was 3.12 ± 1.87 years. Prior to the study visit, the UPDRS-III scores under chronic stimulation were 34.07 ± 11.55 (Stim On/MedOn) (Fig. S1e). Nine patients had unsegmented electrodes, while eight had directional electrodes. In total, we included 449 stimulation combinations from 112 contacts (ring levels). The average VAS score of the training dataset (3.30 ± 2.97) showed a correlation with disease severity, as measured by the UPDRS-III (MED ON/STIM ON) ($R^2 = 0.4634$, $P = 0.0211$) (Fig. S1a). However, no such correlation was observed with the total levodopa equivalent dose (LEED), disease duration, or DBS duration (Figs. S1b–d).

Table 1
Table depicting the sweet and sour spots of our dataset #1, #2, the combined dataset as well as published PD sweet spots from previous work.

MNI Coordinates	X	Y	Z
Right Hemisphere			
Sweet spot (Training Dataset)	13.88 mm	−12.18 mm	−6.08 mm
Sour spot (Training Dataset)	11.68 mm	−15.04 mm	−9.38 mm
Sweet spot (Test Dataset)	14.76 mm	−11.96 mm	−6.08 mm
Sour spot (Test Dataset)	14.76 mm	−15.04 mm	−8.28 mm
Sweet spot (Combined Datasets)	14.10 mm	−11.52 mm	−6.30 mm
Sour spot (Combined Datasets)	13.66 mm	−15.26 mm	−9.60 mm
Sweet Spot Dembek et al.[60]	12.5 mm	−12.72 mm	−5.38 mm
Sweet Spot Horn et al.[62]	12.42 mm	−12.58 mm	−5.92 mm
Left Hemisphere			
Sweet spot (Training Dataset)	−14.06 mm	−13.28 mm	−5.42 mm
Sour spot (Training Dataset)	−11.64 mm	−15.70 mm	−9.16 mm
Sweet spot (Test Dataset)	−15.82 mm	−13.72 mm	−4.54 mm
Sour spot (Test Dataset)	−14.94 mm	−16.80 mm	−6.96 mm
Sweet spot (Combined Datasets)	−14.28 mm	−12.40 mm	−5.86 mm
Sour spot (Combined Datasets)	−13.40 mm	−16.08 mm	−8.94 mm
Sweet Spot Dembek et al.[60]	−12.68 mm	−13.53 mm	−5.38 mm
Sweet Spot Horn et al.[62]	−12.58 mm	−13.41 mm	−5.87 mm

3.2. Sweet spots predict subjective patient feedback

Initially, we analyzed the electrode positioning of the first dataset at the group level (Fig. 1a). To pinpoint anatomical regions linked to positive or negative subjective ratings, we used individual patient electrode positions and VTAs to identify "subjective sweet and sour spots", where "positive" refers to a VAS rating of ≥5 and "negative" refers to a VAS rating <5. Voxel-wise analysis of VAS averages in the anatomical context indicated that the subjective sweet spot was mainly located in the dorsolateral STN, whereas the subjective sour spot was found in the posteroventral STN (Fig. 1b). Anatomical reconstructions showing the center of mass revealed that the VAS sweet spot was situated between the sensorimotor and associative subregions (Fig. 1c). The center of mass for the sweet spots in both hemispheres combined was at MNI coordinates (x, y, z) + 13.88, - 12.18, - 6.08 mm, and the sour spot was at + 11.68, - 15.04, - 9.38 mm. The coordinates of the subjective sweet spot closely matched the previously published sweet spot coordinates by Dembek et al. and Horn et al. [37,40], derived from clinical data (Fig. 1c–Table 2). Analyzing data from 10 cases to predict the remaining 11th case (leave-one-out; cohort 1) demonstrated a positive correlation between the VAS value and the overlap extent of the VTA with the sweet spot map (Fig. 1d) and similar results were obtained from a 5-fold and 10-fold validation as described (Figs. S2a and b) [38]. In summary, we concluded that VTAs stimulating the dorsolateral STN produce the best subjective patient ratings, provided that DBS settings causing significant side effects are excluded.

3.3. Effect of ring level and amplitude in the subjective patient's rating

We hypothesized that electrodes positioned more effectively would yield better VAS ratings. To test this, we calculated the average VAS score for each electrode and identified the respective sweet spots (Fig. S3a). As anticipated, significant differences were observed in the overall distribution of VAS scores for each electrode, with some electrodes showing a bimodal distribution (Fig. S3b). This led us to conclude that subjective patient ratings may partially allow for the differentiation between favorable and unfavorable contacts on a given electrode. To further investigate the correlation between patient ratings and VTA localization, we examined the relationship between VAS values and the ring level for each electrode. We observed a trend towards higher VAS ratings with more dorsal electrode contacts (Fig. S3c). Consistently, higher stimulation amplitudes produced the best VAS ratings at the most dorsal contact level (Fig. S3d). To account for the influence of amplitude size on our data, we analyzed individual sweet spots at various amplitudes (ranging from 0.5 to 3.5 mA). Although the size and shape of sweet spots varied with amplitude, they consistently localized between the sensorimotor and associative STN, in line with our previous findings (Figs. S3e and f). Additionally, examining the impact of stimulation current on VAS ratings across all contacts revealed a peak in VAS ratings at 2–2.5 mA, with ratings decreasing at higher amplitudes. This suggested that stimulation amplitudes between 2 and 2.5 mA were preferred by patients, while higher amplitudes were less favorable

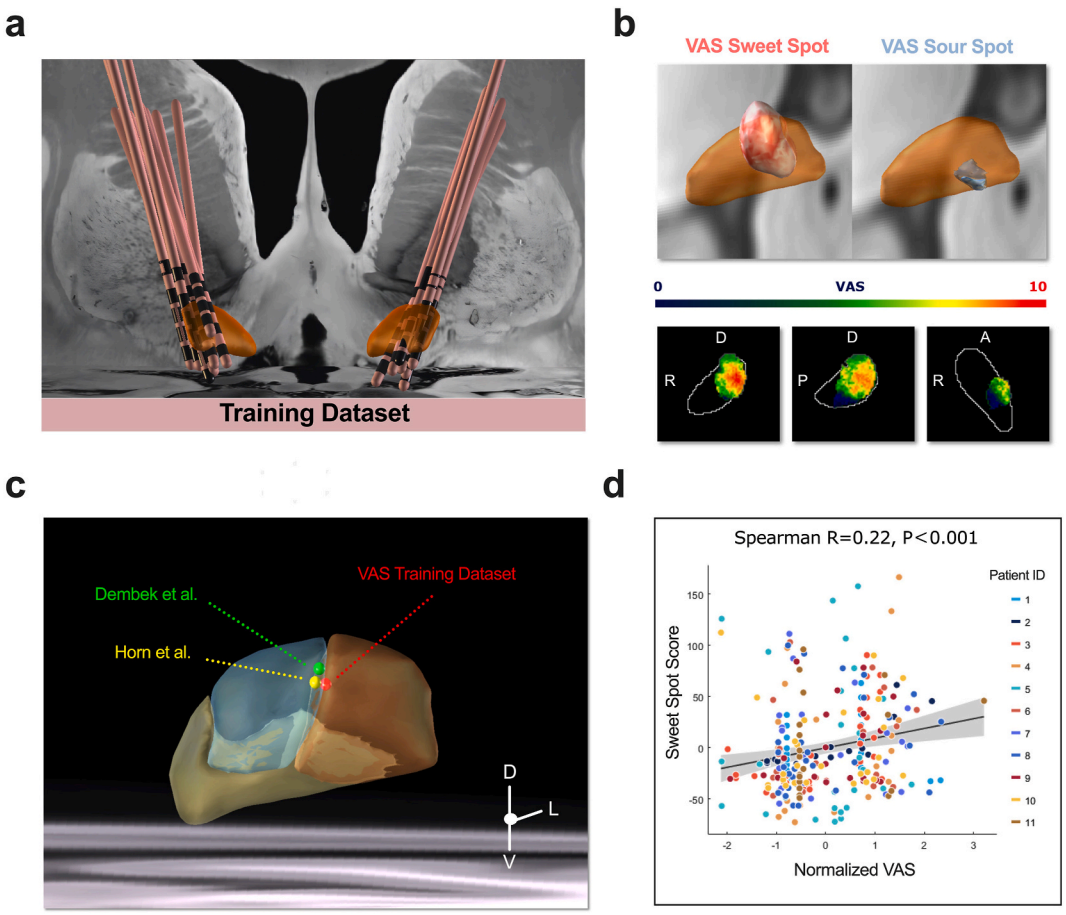

Fig. 1. Subjective sweet spots localize to the dorsolateral STN. (**a**) Group-level electrode reconstructions from the training dataset. (**b**) Upper panel: Images showing the voxel-wise distribution of positively (red) and negatively (blue) rated VTAs across the STN. Lower panel: Heat map illustrating the distribution of VAS ratings in three different anatomical planes. R: Right; D: Dorsal; P: Posterior. (**c**) Graphical representation comparing the center of mass for the subjective sweet spot of the training dataset (red) with sweet spots identified through clinical evaluation (yellow, green). (**d**) Graph displaying a positive correlation between VAS scores and the sweet spot score.

(Fig. S3g).

3.4. Beneficial brain networks predict subjective patient feedback

VTAs are believed to connect to various remote brain networks, which patients may perceive as either favorable or unfavorable. To explore this, we examined the connectome profiles of our subjective sweet spots using whole-brain structural and functional connectivity seeding from bilateral VTAs. Our findings indicated a positive structural connectivity between VTAs with high VAS scores and primary motor cortex (M1) and the supplementary motor area (SMA), and superior frontal gyrus (Fig. 2a), aligning with previous studies that highlighted beneficial structural connectivity in these regions for PD patients [40]. In terms of functional connectivity, we observed positive connectivity with the motor cortex, temporal, and occipital lobes, and negative connectivity with the frontal lobes (Fig. 2b). These models were further validated using a leave-one-cohort-out strategy (x-y-graph inserts: $R = 0.29$, $p < 0.001$ and $R = 0.25$, $p < 0.001$) and confirmed on the Human Connectome Project (HCP) dataset (Figs. S4a and b).

To delve deeper into the relationship between clinical symptoms and patients' subjective experiences, we conducted connectivity analyses on individuals with the most severe and mild symptoms (measured by UPDRS III scores, MED ON/STIM ON) within the entire dataset (Fig. 2c). The structural and functional connectivity maps for the case with the highest UPDRS-III score showed notable differences from the overall maps. Specifically, in terms of structural connectivity, regions that positively correlated with VAS were primarily located in the temporal and parieto-occipital lobes rather than the motor cortex and superior frontal gyrus. Conversely, the case with the lowest UPDRS-III score, connectivity maps were consistent with those of the entire dataset. We then used the highest and lowest VAS scores from the case with the lowest UPDRS-III score to generate the corresponding fiber tract topography (Fig. 2c, right panel). We found that in the case with the low UPDRS-III score, higher VAS scores were associated with more fibers originating from the dorsolateral STN projecting to the SMA and pre-SMA, thereby activating additional brain regions commonly linked to PD improvements, whereas low VAS values indicated a narrower connectivity. These findings, combined with our sweet spot analyses, strongly suggest that patients' subjective ratings can influence clinical outcomes and vice versa.

3.5. Sweet spot and connectivity predict subjective patient ratings in an independent dataset

To validate our findings in an independent dataset, we utilized sweet spot and connectivity data from our training dataset to predict the VAS rating in the test dataset (Fig. 3a). The average VAS score of the test dataset was 3.78 ± 2.46, thus comparable with the training dataset. Following the methodology outlined for the training dataset, we paired VTA measurements with VAS scores, allowing us to identify both subjective sweet- and sour spots within the test dataset and the combined two datasets. Like for the training dataset, the respective sweet spot for

Table 2
Summary table of demographic and device-related characteristics of the study subjects.

ID	Gender	Age Range (yrs.)	Clinically Pre-dominant Side	Frequency (Hz)	Pulse width (μs)	Disease Duration (yrs.)	DBS Duration (yrs.)	UPDRS-III Pre	UPDRS-III Post	Mean LEDD	Mean VAS Score	Clinical Phenotype After DBS Implantation
Dataset #1	11 (3)	61.40 ± 6.2				15.76 ± 2.86	3.29 ± 2.73	34.64 ± 13.04	35.27 ± 11.37	271.5 ± 158.99	3.30 ± 2.97	
01	male	70–75	Left	130	60	16	1	60	56	200	0.16 ± 0.20	H&Y Stage 3 No MF
02	female	55–60	Right	130	60	16	1	52	47	150	1.55 ± 1.30	H&Y Stage 2 Constipation; orthostatic Hypotension; intermittent FOG
03	male	70–75	Right	130	60	18	1	29	32	400	5.35 ± 2.69	H&Y Stage 2.5 Intermittent FOG; slight postural instability
04	male	50–55	Left	130	60	15	3	36	37	400	3.66 ± 3.80	H&Y Stage 2 Constipation; hyposmia No MF
05	male	60–65	Right	130	60	18	4	35	35	200	4.14 ± 1.96	H&Y Stage 2 Orthostatic hypotension No MF
06	female	60–65	Right	130	60	14	5	30	30	610	3.23 ± 3.03	H&Y Stage 1.5 Discrete hyperkinesia 0.5–1.5 h after L-Dopa intake
07	female	60–65	Left	140	60	12	1	25	21	200	3.14 ± 3.33	H&Y Stage 2 FOG 3–4 h after medication
08	male	55–60	Left	140	60	17	5	32	34	255	2.92 ± 3.03	H&Y Stage 2.5 No MF
09	male	55–60	Left	130	60	5	1	11	15	none	4.98 ± 1.78	H&Y Stage 2.5 No MF
10	male	50–55	Left	130	60	15	4	40	43	50	4.42 ± 2.08	H&Y Stage 2.5 Orthostatic hypotension
11	male	55–60	Right	130	60	17	3	31	38	250	1.42 ± 2.67	H&Y Stage 2 No MF
Dataset#2	6 (1)	69.83 ± 5.31				14.33 ± 3.61	4.0 ± 2.0	32.0 ± 3.0	33.33 ± 3.51		3.78 ± 2.46	
01	male	65–70	Left	130	30	19	6	–	–	–	4.25 ± 2.85	n.d.
02	male	70–75	Right	130	60	15	3	–	–	–	5.13 ± 3.64	n.d.
03	male	70–75	Left	130	60	12	3	–	–	–	4.85 ± 1.54	n.d.
04	male	60–65	Right	130	60	18	7	35	37	–	2.38 ± 1.44	n.d.
05	male	70–75	Left	130	40	10	2	29	30	–	2.83 ± 1.57	n.d.
06	female	70–75	Right	130	60	12	3	32	33	–	2.67 ± 2.61	n.d.
Total	17 (4)	63.91 ± 7.62				14.65 ± 3.57	3.12 ± 1.87	34.07 ± 11.55	34.86 ± 10.10		3.50 ± 2.77	

the test dataset was found between the sensorimotor and associative STN regions, while the sour spot was localized to the posteroventral region (Fig. 3b). A comparison with the previously published sweet spot [37,40] suggested that their centers of mass were very close in spatial distribution and ours were slightly dorsal (Fig. 3c–Table 2). To assess the robustness of each subjective sweet spot, we conducted a cross-validation between the datasets. Sweet spots identified from the test dataset were compared with those from the training dataset. The similarity between the groups showed a significant correlation with VAS scores ($R = 0.22$, $p < 0.001$). This exceeded the performance observed during validation on the test dataset ($R = 0.07$, $p = 0.154$). However, analysis of the combined dataset still demonstrated the predictive robustness via leave-one-cohort-out fashion ($R = 0.20$, $p < 0.001$) (Fig. 3d).

Subsequently, we investigated the utility of structural and functional connectivity for cross-validation across datasets. The connectivity patterns identified in the training dataset were applied to predict on test dataset, revealing significant predictive capability for both structural connectivity ($R = 0.13$, $p = 0.033$) and functional connectivity ($R = 0.21$, $p < 0.001$) (Fig. 4a). Moreover, the connectivity patterns, both structural and functional, from VTA sites to distributed brain regions showed high similarity across training dataset, test dataset, and the combined dataset (Fig. 4b) and remained significant with the HPC connectome (Figs. S4c–f). Structural connectivity from the DBS site to the motor cortex and superior frontal gyrus, as well as functional connectivity to the motor cortex, temporal lobes, and occipital lobes, exhibited a positive correlation with VAS scores, while displaying partial negative correlations with functional connectivity to the superior frontal gyrus and middle frontal gyrus. Furthermore, predictions based on the full dataset demonstrated robustness and effectiveness in utilizing patients' subjective ratings as a novel feedback signal for DBS programming, with both structural connectivity ($R = 0.22$, $p < 0.001$) and functional connectivity ($R = 0.23$, $p < 0.001$).

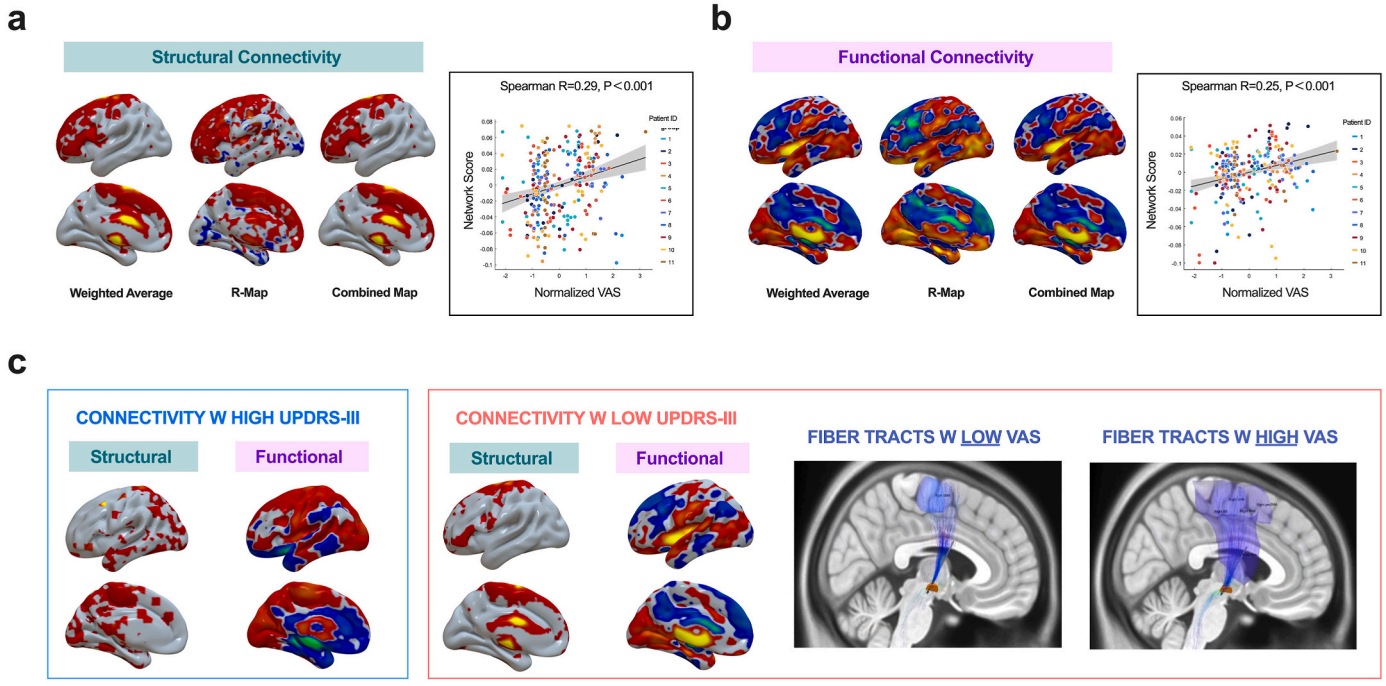

Fig. 2. Patient subjective ratings correlate with beneficial brain network connectivity. (**a,b**) Images depicting structural and functional connectivity maps determined through a weighted average (first column), correlation analysis with VAS (R maps, second column), and a combination of these maps (third column) associated with VAS ratings. Graphs illustrating the correlation of VAS with connectivity; a leave-one-cohort-out approach was used to predict VAS ratings of each patient through the combined map. (**c**) Images illustrating structural and functional connectivity maps (combined maps) of two representative cases with a high or low UPDRS-III score (Med On/Stim On), respectively. Right panel: Topography of the white matter tracts from the case with the lowest UPDRS-III score associated with the highest and lowest VAS values obtained during the study visit.

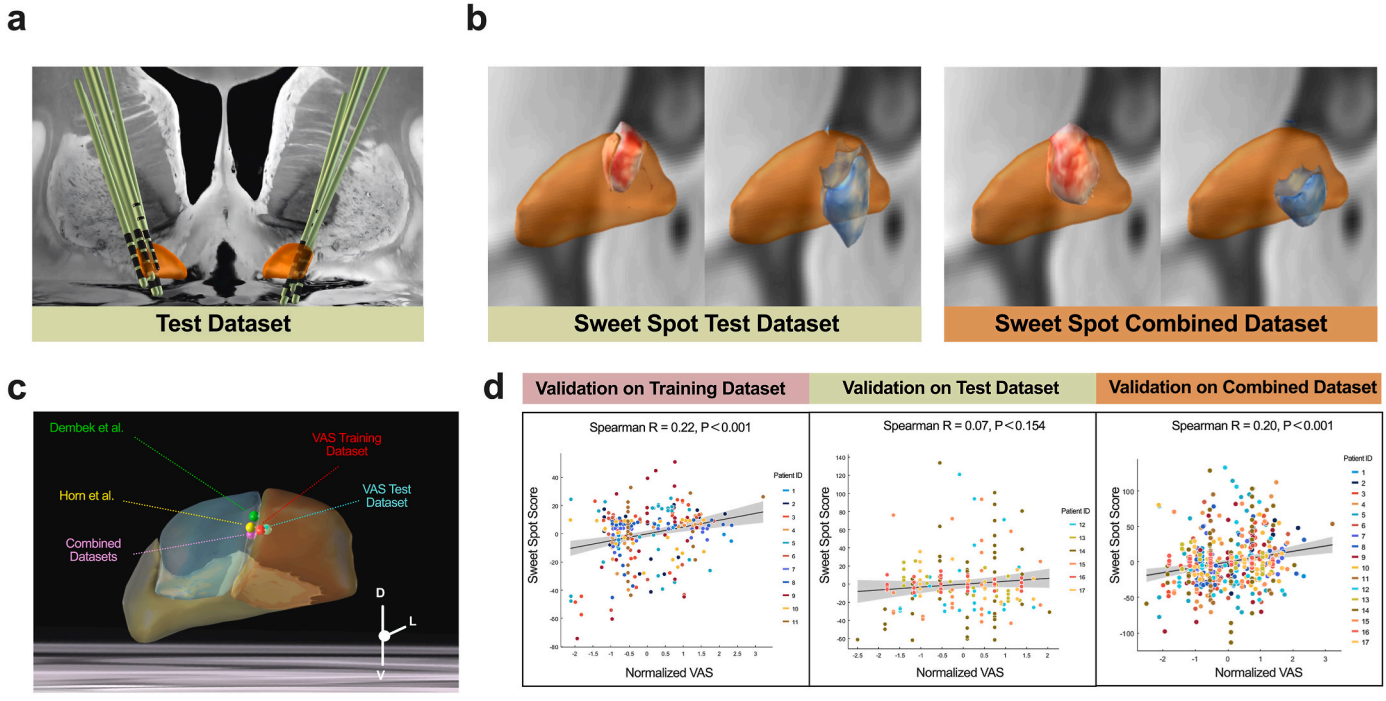

Fig. 3. Validation of VAS based sweet and sour spots in a separate dataset. (**a**) Electrode reconstructions from individual patients in the test dataset (n = 6). (**b**) Images displaying the locations of sweet and sour spots identified in the test dataset (left), as well as those identified when combining data sets (right). (**c**) Illustration comparing the center of mass of sweet spots by MNI coordinates in each dataset with previously published sweet spots [37,40]. (**d**) Graphs demonstrating the predictive accuracy of VAS sweet spots between training and test dataset through cross-validation. Validation on training dataset (left) perform better predictive capability than validation on test dataset (middle). Combined dataset prediction further reveals the robustness of VAS sweet spots predictive capability by leave-one-cohort-out fashion (right).

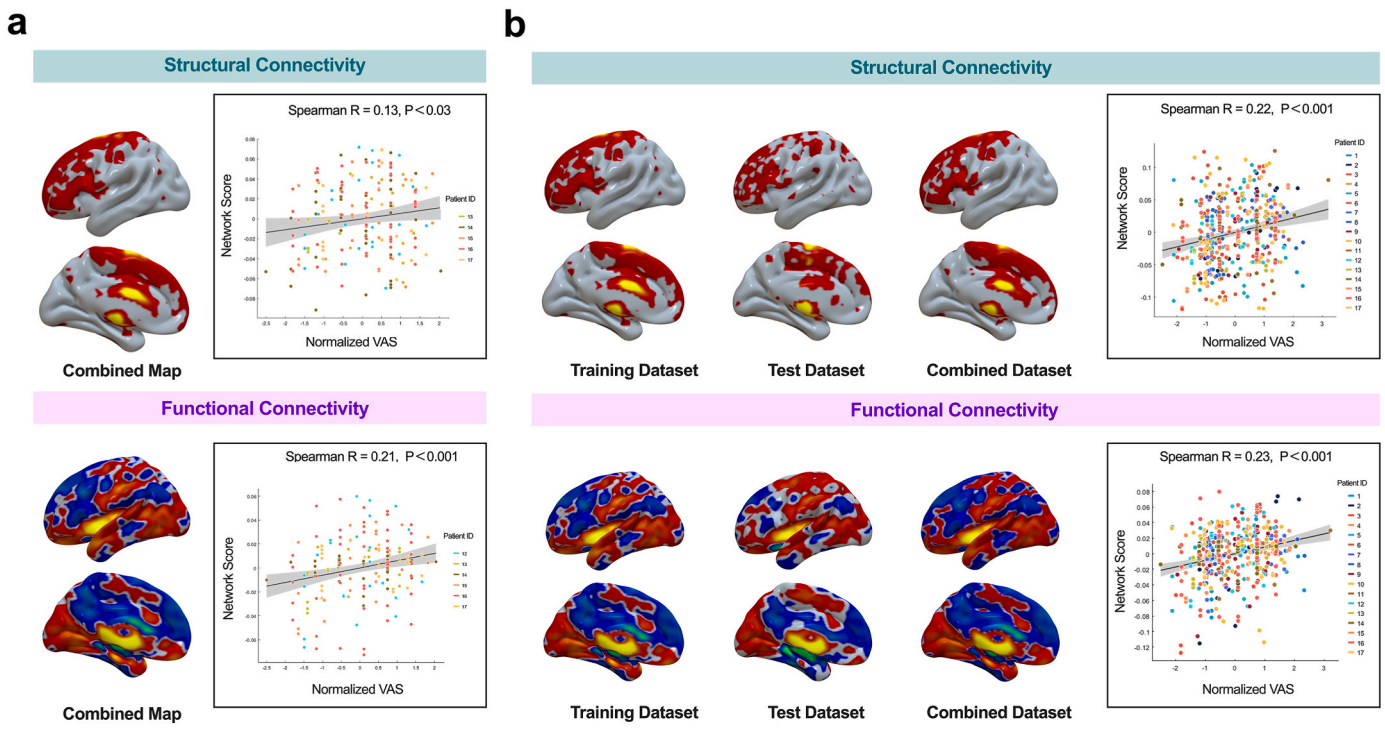

Fig. 4. Validation of VAS based connectivity in a separate dataset. (**a**) Both structural (top) and functional connectivity (bottom) connectivity maps derived from training dataset predict VAS ratings and demonstrate its effectiveness in the independent test dataset. (**b**) The structural (top) and functional connectivity (bottom) profiles identified from training dataset (first column), test dataset (second column) and combined dataset (third column) are all consistent. Statistic graphs (last column) further illustrate the predictive capability of VAS based both structural and functional connectivity by leave-one-cohort-out fashion.

4. Discussion

DBS programming in PD is classically guided by clinical parameters, such as rigor or tremor and has been recently supported by imaging and bioelectrical feedback signals. If a patient's subjective perception or judgement can be helpful for optimizing DBS settings is unclear. Here, we employed advanced imaging analysis in conjunction with psychometric testing to understand which VTAs exhibit the most favorable patient rating and termed thus the subjective sweet spot. Surprisingly, we found that this VAS-based sweet spot localizes to the dorsolateral STN, closely aligning with published sweet spots linked to motor improvement [37,40]. These findings thus underscore the usefulness of patient subjective ratings as a novel feedback signal for effective and well-tolerated DBS programming [43]. Although the correlation was relatively low across the entire dataset, we believe our findings will contribute to the development of VAS-based strategies for DBS programming. Notably, other biomarkers currently under investigation also demonstrate limited predictive value on an individual level. For example, beta-band local field potentials (LFPs) explain only 17 % (R^2) of the individual variability in symptom severity [44].

VAS-based programming routines have the potential to enhance current advancements in DBS programming. For instance, oscillatory activity in the beta frequency band has been suggested as an electrophysiological feedback signal for aDBS, with several studies exploring various closed-loop algorithms utilizing beta-band LFPs [18–25]. However, some reports have questioned the suitability of LFPs as the sole feedback signal for aDBS due to reasons such as the low percentage of explained variability in outcome measures [44–49]. Additionally, the effectiveness of electrophysiological signals can be compromised by incorrect electrode placement in the target area [50]. Misplaced electrodes not only reduce clinical effects and may affect LFP readout accuracy but also contribute to both motor and non-motor side effects of DBS. Even with correct placement in the STN, current projections to other subregions or non-target areas can induce non-motor side effects during chronic STN stimulation [51–58]. A VAS-based programming strategy, which considers patients' subjective perceptions from the outset, could more directly capture these non-motor side effects, thereby improving overall patient satisfaction with DBS treatment. This approach could be further validated by using VAS-based programming as a long-term stimulation parameter and by assessing its impact on quality of life (QoL).

Integrating VAS as a feedback signal into the aDBS system alongside beta frequency data could enhance future developments. Periodic or conditional VAS input would supplement neurophysiological data with patient-reported feedback, enabling real-time, multiparameter adjustments to stimulation. This approach would allow the aDBS system to simultaneously process both objective neurophysiological signals and the patient's subjective experience, thereby optimizing individualized treatment.

The sweet spots identified in our study were predominantly localized to the dorsolateral STN, which is consistent with previous research identifying this area as a common surgical target for STN-DBS in PD [32,37,59]. This alignment underscores the effectiveness of VAS-based adjustment in DBS programming. It is notable that the VAS ratings were obtained within a short period of time after changes in stimulation parameters, suggesting that patients can sense beneficial DBS settings without needing to perform motor tasks or other assessments. VAS ratings may thus be particularly useful for identifying optimal stimulation parameters in settings where clinical examination is not feasible, such as during remote DBS programming [29]. Prospective studies should examine the relevance of VAS-based programming over extended periods as chronic DBS settings.

With cross-validation, sweet spots derived from one dataset showed predictive capability for another dataset, but not the reverse. This discrepancy is likely due to the differing number of data points between the two datasets (11 patients vs. 6 patients), even though both datasets were effective. Moreover, the smaller size of the second dataset might have led to the formation of a larger volume and less variable clusters,

contributing to the observed differences.

Traditionally, surgical planning for DBS has targeted specific sites within the STN. However, recent trends emphasize linking DBS benefits to broader network regulation [40,60]. Notably, recent work suggests that different connectivity patterns are associated with distinct motor symptoms and their therapeutic targeting with DBS [61]. Our results suggest that fiber tracts reaching the STN from the motor cortex positively correlate with subjective patient evaluation, aligning with previous research and highlighting the role of the motor cortex in DBS response [40,62]. Interestingly, we also found a positive association between the M1 and effective STN DBS, which contrasts with some previous studies [40,63,64]. This discrepancy may stem from differences in timing, as VAS captures acute outcomes while previous studies focus on chronic outcomes. Additionally, the subjective nature of VAS encompasses motor and non-motor symptoms, possibly influencing functional networks differently [65]. Our findings support the presence of overlapping stimulation sites within the STN, with different cortical connectivity patterns, associated with improvement in tremor, rigidity and bradykinesia [59,61]. Furthermore, our findings support the existence of potential differences between connectomes associated with clinical outcomes and those linked to subjective patient perceptions, emphasizing their relevance for research aimed at refining DBS programming to address distinct motor symptoms in PD [38,61,66].

5. Limitation

Several limitations of our study should be acknowledged. Notably, the acute nature of the VAS in this study may limit its ability to capture long-term clinical effects, including potential side effects that could emerge over time. VAS may not effectively capture changes in motor symptoms that take longer to manifest, such as bradykinesia or dystonia [67]. Future research, including studies on chronic remote programming, should emphasize long-term efficacy and safety, especially concerning non-motor symptoms, across diverse patient populations and neurological disorder. These studies should consider the clinical reality of misplaced electrodes that appear to occur in 7–17 % of DBS leads [50], with double the risk of at least one electrode being misplaced in bilateral DBS [68]. Our group has explored the applicability of VAS-based programming in a diverse population in the context of the REMOTE trial (NCT05193825), a randomized, prospective, multicenter study evaluating the efficacy and safety of VAS-assisted remote programming. In the REMOTE study, a randomized VAS-based monopolar review was conducted at both the initial (first study visit) and final (second study visit, 90 days post-surgery) time points. This approach aimed to provide study physicians with a standardized summary of the participant's subjective feedback. During remote programming, physicians had the flexibility to use this information for iterative parameter adjustments. While this method may contribute to chronic DBS optimization, further research is needed to explore the practical implementation of chronic VAS programming, potentially as part of an automated machine learning-based approach that integrates repeated VAS feedback into a multi-layer algorithm for DBS parameter refinement. In real-world scenarios, employing such as strategy in conjunction with larger sample sizes would help minimize the impact of outliers, while repeated patient feedback could enhance reliability and robustness.

VAS sampling - like any psychometric research method - is potentially susceptible to confounding by external and internal factors, like for instance fatigue. In the present study, we indeed observed a small trend toward more positive VAS values over time (Fig. S5), suggesting the influence of additional, yet unidentified, confounders on VAS ratings. Although these effects apparently did not influence our main outcome, future studies should systematically examine the impact of such factors (e.g., On vs. Off states) to enhance the reliability of VAS ratings in clinical practice. Finally, we used connectome datasets instead of individual dMRI and fMRI data, which may not fully correspond to individual anatomy. Although we validated our findings using two distinct connectome datasets and across different cohorts, the small sample size and limited clinical diversity—characterized by relatively low LEDD levels and a short time interval since DBS implantation—may restrict the generalizability of our results. This underscores the need for larger studies with a more diverse participant pool. Recruiting a more diverse group of patients across multiple centers, including cases with sub-optimally placed electrodes, could enhance the robustness of our findings and confirm the utility of subjective patient ratings as a feedback signal for DBS programming.

6. Conclusion

Our study suggests that stimulation of the dorsolateral STN, based on subjective patient perception, results in the best patient ratings. These findings indicate that patients can identify beneficial stimulation settings, emphasizing that subjective ratings could be valuable in optimizing DBS programming.

CRediT authorship contribution statement

Jing Dong: Writing – original draft, Visualization, Validation, Software, Project administration, Formal analysis. **Sophia Peschke:** Writing – review & editing, Investigation, Data curation. **Angelina Kirschner:** Writing – review & editing, Validation, Data curation. **Carla Palleis:** Writing – review & editing, Investigation, Conceptualization. **Jan Hinnerk Mehrkens:** Writing – review & editing, Investigation, Data curation. **Maximilian Scherer:** Writing – review & editing, Supervision. **Elisabeth Kaufmann:** Writing – review & editing, Validation, Supervision, Methodology, Conceptualization. **Thomas Koeglsperger:** Writing – review & editing, Writing – original draft, Resources, Project administration, Methodology, Conceptualization.

Data availability

The data that support the findings of this study are available from the corresponding author, upon reasonable request.

Declaration of generative AI and AI-assisted technologies in the writing process

During the preparation of this work, the authors used ChatGPT (Open AI) to correct grammatical and syntactic errors. After using this tool, the authors reviewed and edited the content as needed and take full responsibility for the content of the published article.

Funding

This research was funded by the Munich Advanced Clinician Scientist Program (MCSP) to T.K. and E.K. C.P. was supported by the Deutsche Forschungsgemeinschaft (DFG, German Research Foundation) under Germany's Excellence Strategy within the framework of the Munich Cluster for Systems Neurology (EXC 2145 SyNergy – ID 390857198), the Thiemann Stiftung, Lüneburg Heritage and Friedrich-Baur-Stiftung. M. S. was supported by the Alexander von Humboldt Foundation.

Declaration of competing interest

The authors declare the following financial interests/personal relationships which may be considered as potential competing interests: T. K. reports financial support was provided by Abbott Laboratories. T.K. reports financial support was provided by AbbVie Inc. T.K. reports financial support was provided by Medtronic Inc. T.K. reports a relationship with Abbott Laboratories that includes: funding grants, speaking and lecture fees, and travel reimbursement. T.K. reports a relationship with AbbVie Inc that includes: speaking and lecture fees. T.

K. reports a relationship with Medtronic that includes: funding grants. T. K. is debuty president of the German DBS Association If there are other authors, they declare that they have no known competing financial interests or personal relationships that could have appeared to influence the work reported in this paper.

Acknowledgements

J.D. was supported by the Chinese Scholarship Council (CSC).

Appendix A. Supplementary data

Supplementary data to this article can be found online at https://doi.org/10.1016/j.brs.2025.03.008.

References

[1] Volkmann J, Moro E, Pahwa R. Basic algorithms for the programming of deep brain stimulation in Parkinson's disease. Mov Disord : Official Journal of the Movement Disorder Society 2006;21(Suppl 14):S284–9. https://doi.org/10.1002/mds.20961.
[2] Machado A, Rezai AR, Kopell BH, Gross RE, Sharan AD, Benabid A-L. Deep brain stimulation for Parkinson's disease: surgical technique and perioperative management. Mov Disord : Official Journal of the Movement Disorder Society 2006;21:S247–58. https://doi.org/10.1002/mds.20959.
[3] Okun MS, Tagliati M, Pourfar M, Fernandez HH, Rodriguez RL, Alterman RL, et al. Management of referred deep brain stimulation failures: a retrospective analysis from 2 movement disorders centers. Arch Neurol 2005;62:1250–5. https://doi.org/10.1001/archneur.62.8.noc40425.
[4] Moro E, Poon Y-YW, Lozano AM, Saint-Cyr JA, Lang AE. Subthalamic nucleus stimulation: improvements in outcome with reprogramming. Arch Neurol 2006;63:1266–72. https://doi.org/10.1001/archneur.63.9.1266.
[5] Koeglsperger T, Palleis C, Hell F, Mehrkens JH, Bötzel K. Deep brain stimulation programming for movement disorders: current concepts and evidence-based strategies. Front Neurol 2019;10:410. https://doi.org/10.3389/fneur.2019.00410.
[6] Hunka K, Suchowersky O, Wood S, Derwent L, Kiss ZHT. Nursing time to program and assess deep brain stimulators in movement disorder patients. J Neurosci Nurs : Journal of the American Association of Neuroscience Nurses 2005;37:204–10.
[7] Hell F, Palleis C, Mehrkens JH, Koeglsperger T, Bötzel K. Deep brain stimulation programming 2.0: future perspectives for target identification and adaptive closed loop stimulation. Front Neurol 2019;10:314. https://doi.org/10.3389/fneur.2019.00314.
[8] Pulliam CL, Heldman DA, Orcutt TH, Mera TO, Giuffrida JP, Vitek JL. Motion sensor strategies for automated optimization of deep brain stimulation in Parkinson's disease. Parkinsonism Relat Disord 2015;21:378–82. https://doi.org/10.1016/j.parkreldis.2015.01.018.
[9] Waldthaler J, Bopp M, Kühn N, Bacara B, Keuler M, Gjorgjevski M, et al. Imaging-based programming of subthalamic nucleus deep brain stimulation in Parkinson's disease. Brain Stimul 2021;14:1109–17. https://doi.org/10.1016/j.brs.2021.07.064.
[10] Lange F, Steigerwald F, Malzacher T, Brandt GA, Odorfer TM, Roothans J, et al. Reduced programming time and strong symptom control even in chronic course through imaging-based DBS programming. Front Neurol 2021;12:785529. https://doi.org/10.3389/fneur.2021.785529.
[11] Roediger J, Dembek TA, Wenzel G, Butenko K, Kühn AA, Horn A. StimFit—a data-driven algorithm for automated deep brain stimulation programming. Mov Disord 2022;37:574–84. https://doi.org/10.1002/mds.28878.
[12] Neudorfer C, Kroneberg D, Al-Fatly B, Goede L, Kübler D, Faust K, et al. Personalizing deep brain stimulation using advanced imaging sequences. Ann Neurol 2022;91:613–28. https://doi.org/10.1002/ana.26326.
[13] Vilkhu G, Goas C, Miller JA, Kelly SM, McDonald KJ, Tsai AJ, et al. Clinician vs. imaging-based subthalamic nucleus deep brain stimulation programming. Park Relat Disord 2023;106:105241. https://doi.org/10.1016/j.parkreldis.2022.105241.
[14] Mills KA, Mari Z. Imaging-based DBS programming help: does it help? Park Relat Disord 2023;109:105362. https://doi.org/10.1016/j.parkreldis.2023.105362.
[15] Segura-Amil A, Nowacki A, Debove I, Petermann K, Tinkhauser G, Krack P, et al. Programming of subthalamic nucleus deep brain stimulation with hyperdirect pathway and corticospinal tract-guided parameter suggestions. Hum Brain Mapp 2023;44:4439–51. https://doi.org/10.1002/hbm.26390.
[16] Torres V, Giudice KD, Roldán P, Rumià J, Muñoz E, Cámara A, et al. Image-guided programming deep brain stimulation improves clinical outcomes in patients with Parkinson's disease. Npj Park's Dis 2024;10:29. https://doi.org/10.1038/s41531-024-00639-9.
[17] Rolland A-S, Touzet G, Carriere N, Mutez E, Kreisler A, Simonin C, et al. The use of image guided programming to improve deep brain stimulation workflows with directional leads in Parkinson's disease. J Park's Dis 2024;14:111–9. https://doi.org/10.3233/jpd-225126.
[18] Rosa M, Arlotti M, Marceglia S, Cogiamanian F, Ardolino G, Fonzo AD, et al. Adaptive deep brain stimulation controls levodopa-induced side effects in Parkinsonian patients. Mov Disord 2017;32:628–9. https://doi.org/10.1002/mds.26953.
[19] Rosa M, Arlotti M, Ardolino G, Cogiamanian F, Marceglia S, Fonzo AD, et al. Adaptive deep brain stimulation in a freely moving Parkinsonian patient. Mov Disord : Official Journal of the Movement Disorder Society 2015;30:1003–5. https://doi.org/10.1002/mds.26241.
[20] Little S, Tripoliti E, Beudel M, Pogosyan A, Cagnan H, Herz D, et al. Adaptive deep brain stimulation for Parkinson's disease demonstrates reduced speech side effects compared to conventional stimulation in the acute setting. J Neurol Neurosurg Psychiatr 2016;87:1388–9. https://doi.org/10.1136/jnnp-2016-313518.
[21] Piña-Fuentes D, Dijk JMC van, Zijl JC van, Moes HR, Laar T van, Oterdoom DLM, et al. Acute effects of adaptive deep brain stimulation in Parkinson's disease. Brain Stimul 2020;13:1507–16. https://doi.org/10.1016/j.brs.2020.07.016.
[22] Velisar A, Syrkin-Nikolau J, Blumenfeld Z, Trager MH, Afzal MF, Prabhakar V, et al. Dual threshold neural closed loop deep brain stimulation in Parkinson disease patients. Brain Stimul 2019;12:868–76. https://doi.org/10.1016/j.brs.2019.02.020.
[23] Arlotti M, Marceglia S, Foffani G, Volkmann J, Lozano AM, Moro E, et al. Eight-hours adaptive deep brain stimulation in patients with Parkinson disease. Neurology 2018;90:e971–6. https://doi.org/10.1212/wnl.0000000000005121.
[24] Bocci T, Prenassi M, Arlotti M, Cogiamanian FM, Borellini L, Moro E, et al. Eight-hours conventional versus adaptive deep brain stimulation of the subthalamic nucleus in Parkinson's disease. Npj Park Dis 2021;7:88. https://doi.org/10.1038/s41531-021-00229-z.
[25] Little S, Pogosyan A, Neal S, Zavala B, Zrinzo L, Hariz M, et al. Adaptive deep brain stimulation in advanced Parkinson disease. Ann Neurol 2013;74:449–57. https://doi.org/10.1002/ana.23951.
[26] Jost ST, Sauerbier A, Visser-Vandewalle V, Ashkan K, Silverdale M, Evans J, et al. A prospective, controlled study of non-motor effects of subthalamic stimulation in Parkinson's disease: results at the 36-month follow-up. J Neurol Neurosurg Psychiatr 2020;91:687–94. https://doi.org/10.1136/jnnp-2019-322614.
[27] Nassery A, Palmese CA, Sarva H, Groves M, Miravite J, Kopell BH. Psychiatric and cognitive effects of deep brain stimulation for Parkinson's disease. Curr Neurol Neurosci Rep 2016;16:87. https://doi.org/10.1007/s11910-016-0690-1.
[28] Castrioto A, Lhommée E, Moro E, Krack P. Mood and behavioural effects of subthalamic stimulation in Parkinson's disease. Lancet Neurol 2014;13:287–305. https://doi.org/10.1016/s1474-4422(13)70294-1.
[29] Nie P, Zhang J, Yang X, Shao Y, Zhang X, Liu W, et al. Remote programming in patients with Parkinson's disease after deep brain stimulation: safe, effective, and economical. Front Neurol 2022;13:879250. https://doi.org/10.3389/fneur.2022.879250.
[30] Palleis C, Gehmeyr M, Mehrkens JH, Bötzel K, Koeglsperger T. Establishment of a visual analog scale for DBS programming (VISUAL-STIM trial). Front Neurol 2020;11:561323. https://doi.org/10.3389/fneur.2020.561323.
[31] Hellerbach A, Dembek TA, Hoevels M, Holz JA, Gierich A, Luyken K, et al. DiODe: directional orientation detection of segmented deep brain stimulation leads: a sequential algorithm based on CT imaging. Stereotact Funct Neurosurg 2018;96:335–41. https://doi.org/10.1159/000494738.
[32] Horn A, Li N, Dembek TA, Kappel A, Boulay C, Ewert S, et al. Lead-DBS v2: towards a comprehensive pipeline for deep brain stimulation imaging. Neuroimage 2019;184:293–316. https://doi.org/10.1016/j.neuroimage.2018.08.068.
[33] Husch A, Petersen MV, Gemmar P, Goncalves J, Hertel F. PaCER - a fully automated method for electrode trajectory and contact reconstruction in deep brain stimulation. Neuroimage: Clinica 2018;17:80–9. https://doi.org/10.1016/j.nicl.2017.10.004.
[34] Ewert S, Plettig P, Li N, Chakravarty MM, Collins DL, Herrington TM, et al. Toward defining deep brain stimulation targets in MNI space: a subcortical atlas based on multimodal MRI, histology and structural connectivity. Neuroimage 2017;170:271–82. https://doi.org/10.1016/j.neuroimage.2017.05.015.
[35] Vorwerk J, Cho J-H, Rampp S, Hamer H, Knösche TR, Wolters CH. A guideline for head volume conductor modeling in EEG and MEG. Neuroimage 2014;100:590–607. https://doi.org/10.1016/j.neuroimage.2014.06.040.
[36] Astrom M, Diczfalusy E, Martens H, Wardell K. Relationship between neural activation and electric field distribution during deep brain stimulation. IEEE Trans Biomed Eng 2014;62:664–72. https://doi.org/10.1109/tbme.2014.2363494.
[37] Dembek TA, Roediger J, Horn A, Reker P, Oehrn C, Dafsari HS, et al. Probabilistic sweet spots predict motor outcome for deep brain stimulation in Parkinson disease. Ann Neurol 2019;86:527–38. https://doi.org/10.1002/ana.25567.
[38] Hacker ML, Rajamani N, Neudorfer C, Hollunder B, Oxenford S, Li N, et al. Connectivity profile for subthalamic nucleus deep brain stimulation in early stage Parkinson disease. Ann Neurol 2023;94:271–84. https://doi.org/10.1002/ana.26674.
[39] Marek K, Jennings D, Lasch S, Siderowf A, Tanner C, Simuni T, et al. The Parkinson progression marker initiative (PPMI). Prog Neurobiol 2011;95:629–35. https://doi.org/10.1016/j.pneurobio.2011.09.005.
[40] Horn A, Reich M, Vorwerk J, Li N, Wenzel G, Fang Q, et al. Connectivity Predicts deep brain stimulation outcome in Parkinson disease. Ann Neurol 2017;82:67–78. https://doi.org/10.1002/ana.24974.
[41] Bookheimer SY, Salat DH, Terpstra M, Ances BM, Barch DM, Buckner RL, et al. The lifespan human connectome Project in aging: an overview. Neuroimage 2019;185:335–48. https://doi.org/10.1016/j.neuroimage.2018.10.009.
[42] Kim MJ, Shi Y, Lee J, Salimpour Y, Anderson WS, Mills KA. Anatomical substrates and connectivity for bradykinesia motor features in Parkinson's disease after subthalamic nucleus deep brain stimulation. Brain Commun 2023;5:fcad337. https://doi.org/10.1093/braincomms/fcad337.
[43] Munhoz RP, Albuainain G. Deep brain stimulation: new programming algorithms and teleprogramming. Expert Rev Neurother 2023;23:467–78. https://doi.org/10.1080/14737175.2023.2208749.

[44] Wijk BCM van, Bie RMA de, Beudel M. A systematic review of local field potential physiomarkers in Parkinson's disease: from clinical correlations to adaptive deep brain stimulation algorithms. J Neurol 2023;270:1162–77. https://doi.org/10.1007/s00415-022-11388-1.
[45] Torrecillos F, Tinkhauser G, Fischer P, Green AL, Aziz TZ, Foltynie T, et al. Modulation of beta bursts in the subthalamic nucleus predicts motor performance. J Neurosci 2018;38:8905–17. https://doi.org/10.1523/jneurosci.1314-18.2018.
[46] Ozturk M, Abosch A, Francis D, Wu J, Jimenez-Shahed J, Ince NF. Distinct subthalamic coupling in the on state describes motor performance in Parkinson's disease. Mov Disord 2020;35:91–100. https://doi.org/10.1002/mds.27800.
[47] Rosa M, Marceglia S, Servello D, Foffani G, Rossi L, Sassi M, et al. Time dependent subthalamic local field potential changes after DBS surgery in Parkinson's disease. Exp Neurol 2010;222:184–90. https://doi.org/10.1016/j.expneurol.2009.12.013.
[48] Hill ME, Johnson LA, Wang J, Sanabria DE, Patriat R, Cooper SE, et al. Paradoxical modulation of STN β-band activity with medication compared to deep brain stimulation. Mov Disord 2023. https://doi.org/10.1002/mds.29634.
[49] Kühn AA, Tsui A, Aziz T, Ray N, Brücke C, Kupsch A, et al. Pathological synchronisation in the subthalamic nucleus of patients with Parkinson's disease relates to both bradykinesia and rigidity. Exp Neurol 2009;215:380–7. https://doi.org/10.1016/j.expneurol.2008.11.008.
[50] Rolston JD, Englot DJ, Starr PA, Larson PS. An unexpectedly high rate of revisions and removals in deep brain stimulation surgery: analysis of multiple databases. Parkinsonism Relat Disorders 2016;33:72–7. https://doi.org/10.1016/j.parkreldis.2016.09.014.
[51] Krack P, Kumar R, Ardouin C, Dowsey PL, McVicker JM, Benabid A, et al. Mirthful laughter induced by subthalamic nucleus stimulation. Mov Disord 2001;16:867–75. https://doi.org/10.1002/mds.1174.
[52] Mallet L, Schüpbach M, N'Diaye K, Remy P, Bardinet E, Czernecki V, et al. Stimulation of subterritories of the subthalamic nucleus reveals its role in the integration of the emotional and motor aspects of behavior, vol. 104. Proceedings of the National Academy of Sciences; 2007. p. 10661–6. https://doi.org/10.1073/pnas.0610849104.
[53] Kulisevsky J, Berthier ML, Gironell A, Pascual-Sedano B, Molet J, Parés P. Mania following deep brain stimulation for Parkinson's disease. Neurology 2002;59:1421–4. https://doi.org/10.1212/wnl.59.9.1421.
[54] Romito LM, Raja M, Daniele A, Contarino MF, Bentivoglio AR, Barbier A, et al. Transient mania with hypersexuality after surgery for high frequency stimulation of the subthalamic nucleus in Parkinson's disease. Mov Disord : Official Journal of the Movement Disorder Society 2002;17:1371–4. https://doi.org/10.1002/mds.10265.
[55] Herzog J, Reiff J, Krack P, Witt K, Schrader B, Müller D, et al. Manic episode with psychotic symptoms induced by subthalamic nucleus stimulation in a patient with Parkinson's disease. Mov Disord : Official Journal of the Movement Disorder Society 2003;18:1382–4. https://doi.org/10.1002/mds.10530.
[56] Bejjani BP, Damier P, Arnulf I, Thivard L, Bonnet AM, Dormont D, et al. Transient acute depression induced by high-frequency deep-brain stimulation. N Engl J Med 1999;340:1476–80. https://doi.org/10.1056/nejm199905133401905.
[57] Lazcano-Ocampo C, Wamelen D van, Samuel M, Silverdale M, Rizos A, Sauerbier A, et al. Evaluation of the effect of bilateral subthalamic nucleus deep brain stimulation on fatigue in Parkinson's Disease as measured by the non-motor symptoms scale. Br J Neurosurg 2021:1–4. https://doi.org/10.1080/02688697.2021.1961681.
[58] Witt K, Granert O, Daniels C, Volkmann J, Falk D, Eimeren T van, et al. Relation of lead trajectory and electrode position to neuropsychological outcomes of subthalamic neurostimulation in Parkinson's disease: results from a randomized trial. Brain : J Neurol 2013;136:2109–19. https://doi.org/10.1093/brain/awt151.
[59] Akram H, Sotiropoulos SN, Jbabdi S, Georgiev D, Mahlknecht P, Hyam J, et al. Subthalamic deep brain stimulation sweet spots and hyperdirect cortical connectivity in Parkinson's disease. Neuroimage 2017;158:332–45. https://doi.org/10.1016/j.neuroimage.2017.07.012.
[60] Horn A, Wenzel G, Irmen F, Huebl J, Li N, Neumann W-J, et al. Deep brain stimulation induced normalization of the human functional connectome in Parkinson's disease. Brain : J Neurol 2019;142:3129–43. https://doi.org/10.1093/brain/awz239.
[61] Rajamani N, Friedrich H, Butenko K, Dembek T, Lange F, Navrátil P, et al. Deep brain stimulation of symptom-specific networks in Parkinson's disease. Nat Commun 2024;15:4662. https://doi.org/10.1038/s41467-024-48731-1.
[62] Accolla EA, Ruiz MH, Horn A, Schneider G-H, Schmitz-Hübsch T, Draganski B, et al. Brain networks modulated by subthalamic nucleus deep brain stimulation. Brain : J Neurol 2016;139:2503–15. https://doi.org/10.1093/brain/aww182.
[63] Wang Q, Akram H, Muthuraman M, Gonzalez-Escamilla G, Sheth SA, Oxenford S, et al. Normative vs. patient-specific brain connectivity in deep brain stimulation. Neuroimage 2020;224:117307. https://doi.org/10.1016/j.neuroimage.2020.117307.
[64] Ceballos-Baumann AO, Boecker H, Bartenstein P, Falkenhayn I von, Riescher H, Conrad B, et al. A positron emission tomographic study of subthalamic nucleus stimulation in Parkinson disease: enhanced movement-related activity of motor-association cortex and decreased motor cortex resting activity. Arch Neurol 1999;56:997–1003. https://doi.org/10.1001/archneur.56.8.997.
[65] Shen L, Jiang C, Hubbard CS, Ren J, He C, Wang D, et al. Subthalamic nucleus deep brain stimulation modulates 2 distinct neurocircuits. Ann Neurol 2020;88:1178–93. https://doi.org/10.1002/ana.25906.
[66] Hollunder B, Ostrem JL, Sahin IA, Rajamani N, Oxenford S, Butenko K, et al. Mapping dysfunctional circuits in the frontal cortex using deep brain stimulation. Nat Neurosci 2024;27:573–86. https://doi.org/10.1038/s41593-024-01570-1.
[67] McIntyre CC, Anderson RW. Deep brain stimulation mechanisms: the control of network activity via neurochemistry modulation. J Neurochem 2016;139:338–45. https://doi.org/10.1111/jnc.13649.
[68] Hartmann CJ, Fliegen S, Groiss SJ, Wojtecki L, Schnitzler A. An update on best practice of deep brain stimulation in Parkinson's disease. Ther Adv Neurol Disord 2019;12:1756286419838096. https://doi.org/10.1177/1756286419838096.